

CRITICAL DEBONDING LENGTH IN FRP FLEXURALLY STRENGTHENED RC MEMBERS

S.T. Smith¹ and R.J. Gravina²

¹ Centre for Built Infrastructure Research, University of Technology Sydney, NSW, Australia

² School of Civil and Chemical Engineering, RMIT University, Victoria, Australia

ABSTRACT

Reinforced concrete (RC) beams and slabs bonded with tension face fibre reinforced polymers (FRP) are susceptible to premature failure by intermediate crack (IC) induced debonding, otherwise known as IC debonding, that originates at a flexural crack. Two key parameters needed in the determination of IC debonding are (1) the load required to initiate localised debonding near the base of flexural cracks, and (2) the length of debonded plate required to cause complete loss of load carrying capacity of the FRP-strengthened member. These two parameters are investigated in this paper using a local deformation model previously reported by the authors (Gravina and Smith 2004, Smith and Gravina 2005). A recently published bond-slip relation for the FRP-to-concrete interface (Lu et al. 2005) is used to determine the onset of debonding while the local deformation model is used to investigate the debonded plate length in FRP-strengthened RC cantilever slabs. The results are compared with Chen and Teng's (2001) effective bond length and then recommendations given.

KEYWORDS

FRP, RC beams, debonding, local deformation model.

INTRODUCTION

The flexural strength of reinforced concrete (RC) members such as beams and slabs can be increased by bonding fibre reinforced polymer (FRP) plates to their tension face. Debonding of the FRP before the ultimate moment capacity of the strengthened element is reached has been reported in numerous experimental studies over the past decade (Teng et al. 2002). Debonding that initiates at an intermediate crack (IC) in the beam and then continues to one of the plate ends is referred to as intermediate crack-induced (IC) debonding (Figure 1) with a flexural crack in the beam widely accepted to be the initiator of debonding (Teng et al. 2003). Flexural IC debonding, which is the failure mode being investigated in the current study, is believed to be particularly important for relatively slender members, such as slabs, and members strengthened with a relatively thin FRP plate.

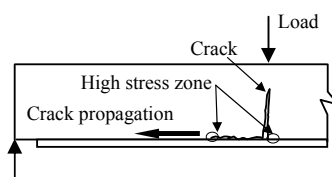


Figure 1 IC debonding

Local deformation models are a particularly powerful tool for analyzing the complete response of FRP-strengthened RC beams from pre- to post-cracking right up to ultimate failure by concrete crushing, FRP rupture or debonding. They allow the formation of flexural cracks to be modelled, as well as associated crack spacing and crack widths. The bond characteristics between the longitudinal steel reinforcement and concrete, and the FRP and concrete, as well as the tension stiffening effect of the reinforcement and FRP to the concrete, are considered, with the non-linear governing equations solved via the finite difference method. Local deformation models thus possess the potential for the IC debonding phenomenon to be investigated in detail.

Existing local deformation based models have been used to investigate the behaviour of FRP strengthened RC members in tension (Ferretti and Savoia 2003) and bending (Ceroni et al. 2001, Aiello and Ombres 2003). None of these models have however considered failure by debonding and in particular IC debonding. Gravina and

Smith (2004) described their own local deformation model that simulated the flexural behaviour of RC flexural members strengthened with a tension face FRP plate that failed by either FRP rupture or concrete crushing. Smith and Gravina (2005) then modified their model to predict IC debonding using Lu et al.'s (2005) FRP-to-concrete bond-slip model to predict the onset of debonding. Cantilevered RC slabs strengthened with tension face FRP that failed by IC debonding initiating at the fixed support, as reported by Yao et al. (2002), were used to confirm the accuracy of the local deformation model with debonding being found to be dependent on and predicted by the FRP-to-concrete bond-slip model.

The current paper extends Smith and Gravina's (2005) study further by investigating the issue of a critical FRP debond length that corresponds to complete loss in load carrying capacity of the strengthened flexural member. Debond lengths of Yao et al.'s (2002) detailed report of FRP-strengthened RC cantilever slabs failing by IC debonding are determined and then compared with Chen and Teng's (2001) effective bond length formula as well as the JSCE (2001) recommendation for considering debonding.

LOCAL DEFORMATION MODEL

A local deformation model was originally presented by Gravina and Warner (2003) for predicting the serviceability and ultimate limit state behaviour of RC beams. The model was later modified to incorporate externally bonded FRP composites for flexural strengthening (Gravina and Smith 2004). A summary of the analytical method for FRP strengthened flexural members is given below and a more comprehensive treatment, as well as simplifying assumptions and governing equations are given in Gravina and Smith (2004). The local deformation model has been found to be in good agreement with test results of FRP flexurally strengthened beams failing by either concrete crushing or FRP rupture (Gravina and Smith 2004).

In summary, the method predicts the local flexural deformations in a determinate structural member at all stages of loading, from progressive formation of individual cracks right up to ultimate failure either by FRP fracture, concrete crushing, or IC debonding. Figure 2 shows a number of discrete blocks bounded by flexural cracks in the cracked region of a FRP-strengthened RC cantilever slab with the uncracked region evident. The strains in the tensile steel reinforcement, FRP strengthening, as well as the slip between the tensile steel and surrounding concrete, and FRP and concrete, are evaluated. The tensile concrete strain between cracks is ignored as it is assumed to be negligible in comparison to the tensile steel and FRP strain. Global deformations such as rotation capacity and deflections can then be determined based on a non-linear analysis.

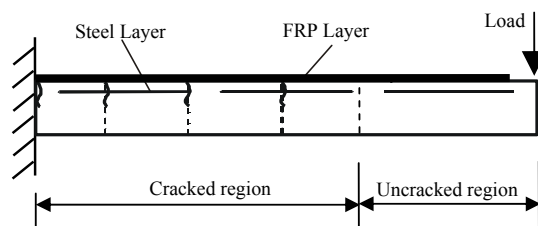


Figure 2 Distribution of cracking in a FRP-strengthened RC cantilever slab

Bond-slip relationships

In order to model local deformations, the bond-slip relations between the steel reinforcement and the surrounding concrete (otherwise known as *steel-to-concrete*), and the FRP plating and adjacent concrete substrate (otherwise known as *FRP-to-concrete*) are required. The following is a summary of the bond-slip relations for the steel-to-concrete and FRP-to-concrete interface adopted in this study.

Steel-to-concrete bond-slip relation

The bond behaviour between the reinforcing steel and concrete is modeled using the well established bond-slip relationship in CEB-FIP (1993). This relation caters for varying degrees of confinement of the concrete, and a reduction in bond stress near the transverse crack implicitly taking into account the effect of steel yielding.

FRP-to-concrete bond-slip relation

Several FRP-to-concrete bond-slip models have been developed over the past decade, with a thorough review given by Yuan et al. (2004) and Lu et al. (2005), however all existing models have been calibrated from the results of lap-shear tests on prismatic concrete specimens with specific geometric and material properties. Such

models are therefore not generic. Lu et al. (2005) recently proposed three generic FRP-to-concrete bond-slip relations of varying complexity, without a significant loss in accuracy between the models, developed from finite element analyses of pull-out tests on FRP-to-concrete bonded joints. They assessed their three models with six previously proposed non-generic bond-slip models against a large database of lap-shear tests and found their models to give the best correlation with test results. Lu et al.'s (2005) simplified bond-slip model, which is neither the most complex or simple model, is adopted in this paper due to its numerical stability when incorporated into the local deformation model. The simplified model is given as follows:

$$\tau = \tau_{max} \sqrt{\frac{s}{s_0}} \quad \text{if } s \leq s_0 \quad (1a)$$

$$\tau = \tau_{max} e^{-\alpha \left(\frac{s}{s_0} - 1 \right)} \quad \text{if } s > s_0 \quad (1b)$$

where $s_0 = 0.0195 \beta_w f_t$, $G_f = 0.308 \beta_w^2 \sqrt{f_t}$, $\alpha = 1 / \left(\frac{G_f}{\tau_{max} s_0} - \frac{2}{3} \right)$, $\tau_{max} = 1.5 \beta_w f_t$, $\beta_w = \sqrt{\frac{2.25 - b_f / b_c}{1.25 + b_f / b_c}}$.

The bond stress and slip are denoted by τ and s respectively, τ_{max} and s_0 are the maximum bond stress and corresponding slip, G_f is the interfacial fracture energy and represents the area under the bond stress - slip curve, β_w is a width ratio factor, and b_f and b_c are the width of the FRP and concrete respectively. The concrete tensile strength is based on the Chinese code for the design of concrete structures (GB 50010 2002) and is given by

$$f_t = 0.395 \left(\frac{f_c}{0.76} \right)^{0.55}, \quad \text{where } f_c \text{ is the concrete cylinder compressive strength.}$$

Figure 3 shows the bond-slip curve according to the Lu et al.'s (2005) simplified model for a concrete tensile strength of 3.1 MPa. This is the concrete tensile strength of one of the test slabs to be later used in this paper.

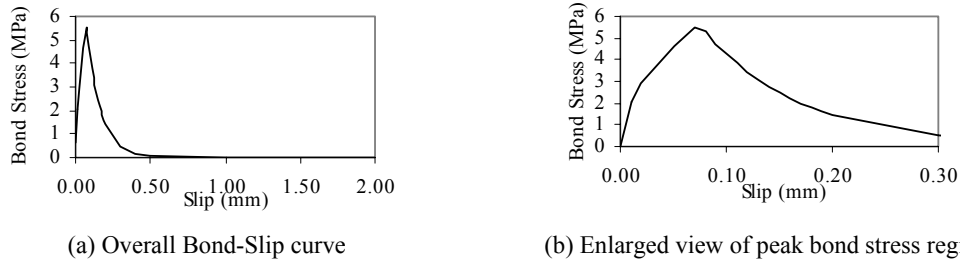


Figure 3 Lu et al.'s (2005) bond slip model for $f_t = 3.1$ MPa

Debonding criteria

There are two key issues to consider when determining the IC debonding resistance of a FRP-strengthened member, namely (1) use of the FRP-to-concrete bond slip model to determine separation of the FRP from the concrete at a discrete position, typically adjacent to flexural cracks in the high moment region, and (2) the critical length of debonded plate for the member as a whole to lose the strength enhancement provided by the FRP. The FRP-to-concrete bond-slip relation is very important as it is used to dictate the onset of debonding. According to Figure 3, just after initial loading chemical breakdown occurs between the concrete and FRP with increased interfacial slip and as a result bond stress increases. Once the peak stress is reached, interfacial softening (or micro-cracking) then starts and the shear (bond) stress reduces with increasing interfacial slip.

Debonding is deemed to occur when a large enough slip has been reached such that minimal bond stress is present. In this paper zero bond stress, which physically means separation of the FRP from the concrete, occurs when the slip is 2 mm (Figure 3a) as verified in Smith and Gravina (2005). When debonding occurs, the analytical solution will yield a solution of constant strain in the FRP between the flexural cracks. The slip between the FRP-to-concrete is in the range of interfacial softening where the bond stress has reduced to zero. Since the bond stress is zero no transfer of strain from the FRP to the concrete substrate can occur therefore leading to no change in the strain in the FRP between flexural cracks.

Anchorage Length of Chen and Teng (2001) and Crack Spacing of JSCE (2001)

The recommendations of Chen and Teng (2001) for effective bond length and JSCE (2001) for crack spacing are compared with the local deformation model predictions in this paper. Chen and Teng (2001) recommended an anchorage length model based on FRP-to-concrete joints under shear. Their effective bond length L_e is given

$$L_e = \sqrt{\frac{E_f t_f}{\sqrt{f'_c}}} \quad (2)$$

where E_f and t_f are the FRP elastic modulus and thickness respectively, and f'_c the concrete cylinder compressive strength. The JSCE (2001) design differentiates between local debonding in the immediate vicinity of a flexural crack in the peak moment region to a critical debond length that spans between adjacent cracks. The crack spacing for use in this model is recommended to be 150–250 mm when the number of layers of FRP is below 3. JSCE (2001) then limits the maximum stress gradient in the plate from the flexural crack at maximum moment (i.e. in the case of a cantilever slab this position is the fixed support) to the next cracking location.

Verification of analytical model with experimental results

The behaviour of a simply supported slab subjected to three-point bending with a span of $2L$ is theoretically the same as a cantilever slab with a cantilever span of L that is subjected to a point load at its free end. The experimental results of Yao et al. (2002) have therefore been used in this paper. The experimental program of Yao et al. (2002) involved the testing of FRP tension face strengthened RC cantilevered slabs that were loaded at their free end. All plates were anchored into the fixed support and all slabs failed by IC debonding that initiated at or near the peak moment position at the fixed support and then extended to the free end of the plate. In the majority of cases debonding at the FRP-to-concrete interface took place in the concrete and this was confirmed by a thin layer of concrete remaining attached to the FRP upon debonding. Smith and Gravina (2005) showed the local deformation model to correlate reasonably well with Yao et al.'s (2002) slabs that failed by IC debonding by using the bond-slip behaviour of the FRP-to-concrete interface to predict debonding.

CRITICAL DEBONDING LENGTH

The critical debonding length of Yao et al.'s (2002) cantilever slabs CP1, CP2, CP3, and CP5 are calculated using the local deformation model in this paper. Geometric and material property details of the slabs are given in Figure 4 and Table 1. In Table 1, b_c and D refer to the width and total depth of the slab respectively, f'_c the concrete cylinder compressive strength, d_s and A_s the depth to the internal tension steel reinforcement from the compressive face and the corresponding tension steel cross-sectional area, and f_{sy} and E_s the yield strength and modulus of elasticity of the steel reinforcement respectively. The thickness and width of the pultruded carbon FRP plate is denoted by t_f and b_f respectively, while the rupture strength and modulus of elasticity of the FRP are denoted by f_f and E_f respectively. The reported peak load at debonding, $P_{db,exp}$ and the associated maximum strain in the FRP at or near the fixed support $\varepsilon_{db,exp}$ are also presented in addition to the strain in the FRP $\varepsilon_{db,anal}$ at the fixed end of the cantilever slab back-calculated from the debonding moment (based on $P_{db,exp}$) using the section analysis fully described in Teng et al. (2002).

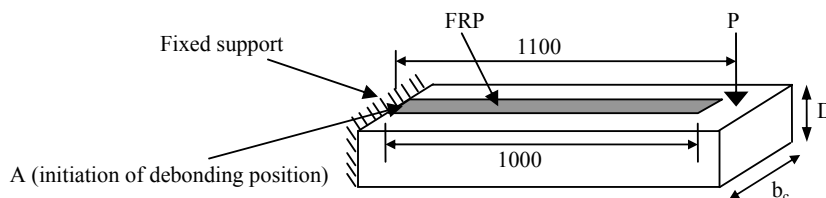


Figure 4 Details of Yao et al.'s (2002) test slabs

To demonstrate the variation in debond length for the slabs given in Table 1, the results of the simulation are presented at three stages of loading namely, (1) at the onset of debonding (i.e. zero bond stress at the first crack positions at the fixed support which translates to localised debonding adjacent to the crack face), (2) debonding having occurred over one cracked block region (i.e. debonding between the crack at the fixed support to the adjacent crack), and (3) debonding in accordance with the reported debond load $P_{db,exp}$ from the experimental tests.

Debond Length for Slab CP1

Due to space limitations, only the complete results for slab CP1 will be given in this paper while a summary of results for slabs CP2, CP3 and CP5, as well as CP1, will be given in the following section. Figures 5 and 6 show

the distributions of strain and bond stress in the FRP along the length of the slab at the three stages of loading for slab CP1, with the typical crack pattern for the cantilever slab shown in Figure 2.

Table 1. Cantilever slab geometric and material properties (Yao et al. 2002)

| Slab | Concrete ^a | | Steel | | | FRP | | | | Debond Load and Strains | | |
|------|-----------------------|------------------------------|-----------------------------|-------------------|----------------|---------------|---------------|----------------|----------------|-------------------------|--|---|
| | d_s (mm) | f'_c (MPa) ^b | A_s (mm ²) | f_{sy} (MPa) | E_s (GPa) | t_f (mm) | b_f (mm) | f_f (MPa) | E_f (GPa) | $P_{db,exp}$ (kN) | $\epsilon_{db,exp}$ ($\mu\epsilon$) | $\epsilon_{db,anal}$ ($\mu\epsilon$) |
| CP1 | 117.4 | 27.0 | 314 | 343 | 208 | 1.2 | 50 | 2800 | 165 | 19.95 | 5420 | 6350 |
| CP2 | 111.3 | 37.7 | 314 | 343 | 208 | 1.2 | 50 | 2800 | 165 | 17.58 | 4298 | 4780 |
| CP3 | 108.2 | 12.6 | 157 | 343 | 208 | 1.2 | 50 | 2800 | 165 | 13.31 | 5240 | 6438 |
| CP5 | 117.4 | 25.6 | 157 | 355 | 210 | 1.2 | 50 | 2800 | 165 | 10.00 | 3761 | 2913 |

^a nominal $b_c = 300$ mm, nominal $D = 150$ mm

^b Converted from tested cube strength using $f'_c = 0.8f_{cu}$

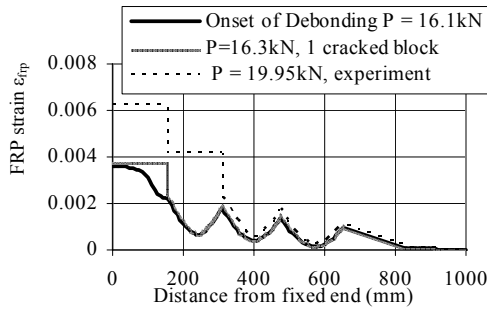


Figure 5 FRP strain distribution

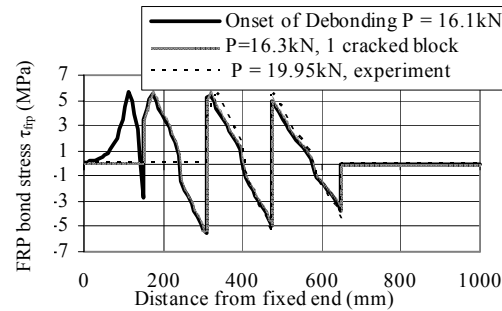


Figure 6 FRP bond stress distribution

Constant FRP strain in Figure 5 signifies a debonded plate. At the onset of debonding the bond stress in Figure 6 is zero at the first crack position (i.e. at the fixed support). At a load of 16.3 kN debonding has quickly progressed and the bond stress is zero over the length of the first cracked block region approximately equal to 150 mm (which is also the crack spacing). At the measured debonding load $P_{db,exp}$ of 19.95 kN, Figure 5 shows FRP debonding extending over 2 cracked block regions and hence the debond length is now 310 mm.

Comparison of Debond Lengths for all Slabs

Tables 2, 3 and 4 are summaries of the debond length L_{debond} determined from the local deformation model for the three stages of loading, as well as the corresponding applied load and strain in the FRP at the fixed end. For ease of comparison the experimental debond applied load and fixed end FRP strain and back-calculated strain are also included. In addition, Chen and Teng's (2001) effective length calculated from Eq. 2 is also included.

The load required to initiate debonding (Table 2) near the fixed end crack to that required to debond one whole cracked block (Table 3) were virtually the same, thus indicating the initial rapid development of debonding. Final debonding occurred at a load higher than that required to debond one whole cracked block. The final debonding length based on the experimental debonding load is given in Table 4 and for slabs CP1, CP2 and CP3 this debond length ranged from approximately one to two times Chen and Teng's (2001) effective bond length (i.e. $L_e < L_{debond} < 2L_e$). The strain in the FRP at debonding derived from the local deformation mode ϵ_{frp} in Table 4 is very similar to the back-calculated strain $\epsilon_{db,anal}$ as to be expected. If the experimental strain near the fixed end $\epsilon_{db,exp}$ is used to drive the analysis then L_{debond} will be less than the L_{debond} given in Tables 3 and 4 which was driven by the experimental debonding load.

Debonding of slab CP5 initiated at a load of 11 kN which was above the experimental debonding load of 10.00 kN. It failed earlier than expected, did not behave as expected, and therefore cannot be explained in this paper. The JSCE (2001) recommendation of crack spacing 150 mm to 250 mm appears to be reasonable based on the crack spacing evident in Figures 5 and 6.

CONCLUSIONS

A local deformation model has been used to determine the critical debond length in FRP-strengthened RC cantilever slabs. The length of debonded plate has been calculated to approximately lie within the range of one to two times the Chen and Teng (2001) recommendation for effective bond, i.e. $L_e < L_{debond} < 2L_e$.

Table 2 Load stage at the onset of debonding

| Slab | Experimental Debond Load and Strains | | | Local Deformation Model Prediction | | | | L_e (Chen & Teng 2001) (mm) |
|------|--------------------------------------|--|---|------------------------------------|-----------|---------------------------------------|----------------------|----------------------------------|
| | $P_{db,exp}$ (kN) | $\epsilon_{db,exp}$ ($\mu\epsilon$) | $\epsilon_{db,anal}$ ($\mu\epsilon$) | Region of Debonding | Load (kN) | ϵ_{frp} ($\mu\epsilon$) | L_{debond} (mm) | |
| CP1 | 19.95 | 5420 | 6350 | Adjacent to crack | 16.1 | 3603 | < 5 | 195 |
| CP2 | 17.58 | 4298 | 4780 | Adjacent to crack | 15.9 | 3745 | < 5 | 180 |
| CP3 | 13.31 | 5240 | 6438 | Adjacent to crack | 10.8 | 3263 | < 5 | 236 |
| CP5 | 10.00 | 3761 | 2913 | Adjacent to crack | 10.8 | 3527 | < 5 | 198 |

Table 3 Load stage according to debonding over 1 cracked block region

| Slab | Experimental Debond Load and Strains | | | Local Deformation Model Prediction | | | | L_e (Chen & Teng 2001) (mm) |
|------|--------------------------------------|--|---|------------------------------------|-----------|---------------------------------------|----------------------|----------------------------------|
| | $P_{db,exp}$ (kN) | $\epsilon_{db,exp}$ ($\mu\epsilon$) | $\epsilon_{db,anal}$ ($\mu\epsilon$) | Region of Debonding | Load (kN) | ϵ_{frp} ($\mu\epsilon$) | L_{debond} (mm) | |
| CP1 | 19.95 | 5420 | 6350 | 1 cracked block | 16.3 | 3603 | 150 | 195 |
| CP2 | 17.58 | 4298 | 4780 | 1 cracked block | 16.1 | 3891 | 155 | 180 |
| CP3 | 13.31 | 5240 | 6438 | 1 cracked block | 11.0 | 3418 | 240 | 236 |
| CP5 | 10.00 | 3761 | 2913 | 1 cracked block | 11.0 | 3661 | 200 | 198 |

Table 4 Load stage according to experimental debond load, $P_{db,exp}$

| Slab | Experimental Debond Load and Strains | | | Local Deformation Model Prediction | | | | L_e (Chen & Teng 2001) (mm) |
|------|--------------------------------------|--|---|------------------------------------|-----------|---------------------------------------|----------------------|----------------------------------|
| | $P_{db,exp}$ (kN) | $\epsilon_{db,exp}$ ($\mu\epsilon$) | $\epsilon_{db,anal}$ ($\mu\epsilon$) | Region of Debonding | Load (kN) | ϵ_{frp} ($\mu\epsilon$) | L_{debond} (mm) | |
| CP1 | 19.95 | 5420 | 6350 | 2 cracked block | 19.95 | 6210 | 310 | 195 |
| CP2 | 17.58 | 4298 | 4780 | 1 cracked block | 17.58 | 4770 | 155 | 180 |
| CP3 | 13.31 | 5240 | 6438 | 2 cracked block | 13.3 | 6298 | 485 | 236 |
| CP5 | 10.00 | 3761 | 2913 | Onset of debond | 10.00 | 2992 | - | 198 |

REFERENCES

- Aiello, M.A. and Ombres, L. (2003) "A model to predict the structural behaviour of reinforced concrete beams strengthened with externally bonded composite sheets", Ed. M.C. Forde, *Proceedings, Tenth International Conference and Exhibition on Structural Faults and Repair-2001; (CD Rom) International Symposium*, London, UK, 1-3 July 2003.
- CEB-FIP (1993) *Model Code for Concrete Structures*, CEB Bulletin d'Information, Comité Euro International du Béton, Lausanne.
- Ceroni, F., Manfredi, G. and Pecce, M. (2001) "Crack widths in RC beams strengthened with carbon fabrics", Ed. C.J. Buyogoyne, *Proceedings, Fifth International Conference on Fibre-Reinforced Plastics for Reinforced Concrete Structures, FRPRCS-5*, Cambridge, UK, 16-18 July, pp. 917-926.
- Chen, J.F. and Teng, J.G. (2001) "Anchorage strength models for FRP and steel plates bonded to concrete", *Journal of Structural Engineering, ASCE*, Vol. 127, No. 7, pp. 784-791.
- Ferretti, D. and Savoia, M. (2003) "Non-linear model for R/C tensile members strengthened by FRP-plates", *Engineering Fracture Mechanics*, Vol. 70, pp. 1069-1083.
- GB 50010 (2002) *Code for Design of Concrete Structures*, Building Industry Press, Beijing, China.
- Gravina R.J. and Warner, R.F. (2003) "Local deformation model for reinforced concrete members in flexure", *Australian Journal of Structural Engineering*, Vol. 5, No. 1, pp. 29-36.
- Gravina, R.J. and Smith, S.T. (2004) "Prediction of flexural behaviour of fibre reinforced polymer strengthened RC beams using a local deformation model", *Proceedings, 18th Australasian Conference on the Mechanics of Structures and Materials, ACMSM 18*, Eds. A.J. Deeks and H. Hao, Perth, Australia, pp. 85-91.
- JSCE (2001) *Recommendations for Upgrading of Concrete Structures with Use of Continuous Fiber Sheets*, Concrete Engineering Series 41 (English version), Japan Society of Civil Engineers (JSCE), Tokyo, Japan.
- Lu, X.Z., Ye, Y.P., Teng, J.G. and Jiang, J.J. (2005) "Meso-scale finite element model for FRP sheets/plates bonded to concrete", *Engineering Structures*, Vol. 27, pp. 564-575.
- Smith, S.T. and Gravina, R.J. (2005) "Prediction of debonding failure in FRP flexurally strengthened RC members using a local deformation model", *submitted for publication*.
- Teng, J.G., Chen, J.F., Smith, S.T. and Lam, L. (2002) *FRP-Strengthened RC Structures*, John Wiley & Sons, Chichester, West Sussex, UK.
- Teng, J.G., Smith, S.T., Yao, J. and Chen, J.F. (2003) "Intermediate crack-induced debonding in RC beams and slabs", *Construction and Building Materials*, Vol. 17, No. 6-7, pp. 447-462.
- Yao, J. Teng, J.G. and Lam, L. (2002) "Debonding in RC cantilever slabs strengthened with FRP strips", Eds. R.A. Sheno, S.S.J. Moi and L.C. Hollaway, *Proceedings, Advanced polymer Composites for Structural Applications in Construction*, Southampton University, UK, 15-17 April 2002, pp. 125-133.
- Yuan, H., Teng, J.G., Seracino, R., Wu, Z.S. and Yao, J. (2004) "Full-range behaviour of FRP-to-concrete bonded joints: A closed form analytical solution", *Engineering Structures*, Vol. 26, pp. 553-565.